

Percolative phase transition on ferromagnetic insulator manganites: uncorrelated to correlated polaron clusters

A.M.L. Lopes,^{1,2,*} J.P. Araújo,³ J.J. Ramasco,⁴ E. Rita,^{1,5} V.S. Amaral,²
J.G. Correia,^{1,5} R. Suryanarayanan,⁶ and the ISOLDE Collaboration¹

¹CERN EP, CH 1211 Geneva 23, Switzerland.

²Departamento de Física and CICECO, Universidade de Aveiro, 3810-193 Aveiro, Portugal.

³Departamento de Física and IFIMUP, Universidade do Porto, 4169-007 Porto, Portugal.

⁴Physics Department, Emory University, Atlanta GA 30322 USA.

⁵ITN, E.N. 10, 2686-953 Sacavém, Portugal.

⁶Laboratoire de Physico-Chimie et de l'Etat Solide, Université Paris-Sud, 91405 Orsay, France.

(Dated: March 22, 2022)

In this work, we report an atomic scale study on the ferromagnetic insulator manganite $\text{LaMnO}_{3.12}$ using $\gamma - \gamma$ PAC spectroscopy. Data analysis reveals a nanoscopic transition from an undistorted to a Jahn–Teller–distorted local environment upon cooling. The percolation thresholds of the two local environments enclose a macroscopic structural transition (Rhombohedral–Orthorhombic). Two distinct regimes of JT–distortions were found: a high temperature regime where uncorrelated polaron clusters with severe distortions of the Mn^{3+}O_6 octahedra survive up to $T \approx 800\text{ K}$ and a low temperature regime where correlated regions have a weaker JT–distorted symmetry.

PACS numbers: 75.47.Lx, 76.80.+y, 64.60.Ak, 31.30.Gs

Intense experimental and theoretical work has been devoted to manganite systems due to their colossal magnetoresistance (CMR), polaron dynamics and charge/orbital ordering phenomena. The undoped manganites (AMnO_3 where A is a trivalent ion of La, Pr, ...) typically show antiferromagnetic insulator behavior and cooperative Jahn–Teller (JT) distortion of MnO_6 octahedra. Oxygen excess or the presence of divalent ions at A–sites reduce the static JT–distortion by the creation of Mn^{4+} ions. This effect favors the ferromagnetic interaction via dynamic electron transfer between Mn^{3+} and Mn^{4+} , the so called double-exchange (DE) interaction [1]. Although DE interaction explains qualitatively the CMR, it does not fully account for the large resistivity of the paramagnetic and ferromagnetic insulator phases. Polaron formation must certainly play an important role in this respect [2, 3, 4, 5]. Polarons are formed due to the strong electron–lattice coupling that leads to charge localization via JT–distortions. Recently, the nature of such local distortions, their dynamics and correlations have been addressed by several authors [6, 7, 8, 9, 10]. In spite of such an effort, several issues as the detailed structure of polarons, the temperature evolution of polaron clusters or the effect of such evolution on the average macroscopic lattice structure still remain as open questions.

Local distortions and their dynamics can be studied by using $\gamma - \gamma$ Perturbed Angular Correlation spectroscopy (PAC), a nuclear hyperfine method specially effective to sample atomic scale environments. PAC efficiency is T independent, allowing to explore a wide range of temperatures. To gain further insight on the microscopic nature of polaronic distortions, their spatial correlations and the role of polarons in ferromagnetic insu-

lator manganites (FMI), we have studied in detail the compound $\text{LaMnO}_{3.12}$ using PAC technique. This compound is a prototypical FMI manganite that undergoes a Rhombohedral (R)-Orthorhombic (O) structural transition around room temperature, which provides us with an ideal scenario to probe the evolution of local lattice distortions through different average lattice symmetries. In particular, we show that random distributed polaron clusters survive in the undistorted R phase up to temperatures as high as 766 K . These distortions are as strong as those observed in the orbital ordered LaMnO_3 . Lowering T , the clusters continuously expand until a microscopic transition takes place at $T_s \approx 170\text{ K}$. Below the transition, the distortions are accommodated into a weaker JT–distorted phase.

$\text{LaMnO}_{3+\Delta}$ polycrystalline samples ($\Delta = 0, 0.08$ and 0.12) were produced by the solid state reaction method. Powder x-ray diffraction measurements show that the samples are chemically homogeneous. In agreement with Refs. [11, 12], we find an antiferromagnetic insulator ground state for the orthorhombic JT–distorted $\Delta = 0$ compound ($T_N \approx 139\text{ K}$), a ferromagnetic insulator behavior for the weakly distorted $\Delta = 0.08$ sample ($T_c \approx 150\text{ K}$) and a ferromagnetic insulator state for the compound with $\Delta = 0.12$ ($T_c \approx 145\text{ K}$). This latter system presents as well an O - R phase transition around room temperature. As shown in Refs. [11, 13], the oxygen excess Δ results in equivalent amounts of La and Mn vacancies, with the fraction of Mn^{4+} equal to 2Δ . $\gamma - \gamma$ PAC measurements were performed using a high-efficiency 6-BaF₂ detector spectrometer [14]. PAC samples (one per measurement) were implanted at room temperature with $^{111\text{m}}\text{Cd}$ to a homogeneous low dose of 10^{12} cm^{-2} at 60 keV in the ISOLDE/CERN facility. Re-

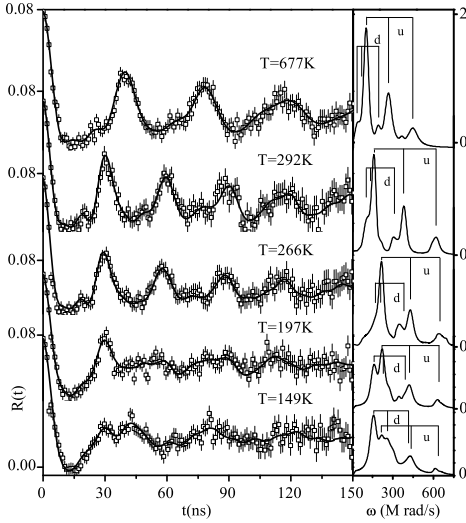


FIG. 1: Representative $R(t)$ experimental functions and the correspondent fits for $\text{LaMnO}_{3.12}$. Corresponding Fourier transforms are displayed on the right side.

maintaining point defects created during implantation were eliminated by annealing at 700°C under O_2 controlled atmosphere for 20 minutes. The peak density of probing Cd only attains 1 ppm of the La concentration. Consequently, the implanted Cd atoms are simply incorporated into La vacancies. The perovskite A (La) site is specially appropriate to detect lattice distortions in the surrounding MnO_6 octahedra since slight changes in the charge geometry will significantly alter the EFG parameters.

The $^{111\text{m}}\text{Cd}$ probes decay to ^{111}Cd through an intermediate state by the emission of two consecutive γ rays. The half life for the $^{111\text{m}}\text{Cd}$ isomeric state is $T_{1/2} = 48\text{ min}$, while for the intermediate state is $T_{1/2} = 84\text{ ns}$. The angular correlation between the two γ rays can be perturbed by both the EFG and the Magnetic Hyperfine Field (MHF). These fields respectively couple to the nuclear electric quadrupole (Q) and the magnetic dipole ($\vec{\mu}$) moments of the intermediate nuclear state. The Hamiltonian for such static interactions, in the proper reference frame of the EFG tensor V_{ij} with $|V_{zz}| \geq |V_{yy}| \geq |V_{xx}|$, reads

$$\mathcal{H} = \frac{\hbar\omega_0}{6} \left[3I_z^2 - I(I+1) + \frac{1}{2}\eta(I_+^2 + I_-^2) \right] + \vec{\mu} \cdot \vec{B}_{hf}, \quad (1)$$

where $\omega_0 = 3eQV_{zz}/(2I(2I-1)\hbar)$ is the fundamental precession frequency, I represents the nuclear spin of the probe intermediate state ($I = 5/2$ for ^{111}Cd), $\eta = (V_{xx} - V_{yy})/V_{zz}$ is the EFG asymmetry parameter and \vec{B}_{hf} is the magnetic hyperfine field [15]. The perturbation of the $\gamma - \gamma$ directional correlation is described by the experimental $R(t)$ function, where t is the time spent by the nucleus in the ^{111}Cd intermediate state. For a hyperfine interaction, $R(t)$ may be expanded as

$R(t) = \sum A_{kk} G_{kk}(t)$ with A_{kk} being the angular correlation coefficients. The perturbation factor $G_{kk}(t)$ is the signature of the fields interacting with the probes: MHF and a EFG in the ferromagnetic phase and EFG alone for $T > T_c$. Below T_c , in the presence of the two fields, we apply combined interaction theory to obtain the MHF and EFG parameters. Above T_c , on the other hand, $G_{kk}(t)$ may be expressed as [15]

$$G_{kk}(t) = S_{k_0} + \sum_n S_{k_n} \cos(\omega_n t) e^{-\omega_n \delta t} \quad (2)$$

considering only pure electric quadrupole interactions. The frequencies ω_n and amplitudes S_{k_n} are determined by the \mathcal{H} diagonalization. For spin $I = 5/2$, three frequencies are observable that are function of ω_0 and η [16]. The exponential term in equation (2) accounts for an attenuation of the $R(t)$ function that appears in all spectra. This effect is due to randomly distributed intrinsic vacancies and defects that produce a Lorentzian distribution of static EFGs with central value ω_0 and relative width δ . Independently, in manganites, short-range charge diffusion coupled to lattice distortions (polarons) can lead to EFG fluctuations. These fluctuations contribute to further attenuate $R(t)$ when their time scale is comparable to the life time of the PAC probe intermediate state. When the characteristic fluctuation time (τ) is shorter than the nuclear spin precession time ($2\pi/\omega_0$), the $R(t)$ function can be satisfactorily approximated by a single exponential damping term $e^{-\lambda t}$ multiplying the static expression (2) with $\lambda \propto \omega_0^2 \tau$ [17].

Some experimental $R(t)$ curves are displayed in Fig. 1 for the compound with $\Delta = 0.12$. We find in the temperature range from 10 K to 766 K the coexistence of three main local environments (u, d, r), *i.e.* three fractions of probes (f_u, f_d, f_r) interacting with different local EFG distributions. The environment r is detected by a low residual fraction of the Cd probes (5%), which is temperature independent. Its EFG parameters are approximately $V_{zz}^r \approx 102\text{ V/\AA}^2$ and $\eta_r \approx 0.9$ at room temperature. These values suggest a very asymmetric local charge distribution. The origin of this environment might be related to probes located at the vicinity of Mn/La vacancies and/or other defects. Actually, assuming that the positions of the vacancies are not correlated, the probability that a Cd siting in a La vacancy has in its surrounding a Mn or next shell La vacancies is roughly 2%.

In Fig.2, the temperature dependence of the EFG asymmetry parameter η (top) and principal component V_{zz} (bottom) for the u and d environments is displayed. For comparison, the EFG parameters found in $\Delta = 0.08$ and $\Delta = 0$ samples are also included in the same figure. The u environment that is dominant at high T shows an almost axially symmetric EFG ($\eta_u \approx 0$). This value characterizes an EFG with an axis of threefold or higher rotational symmetry, which is compatible with the Rhombohedral lattice structure observed at high tem-

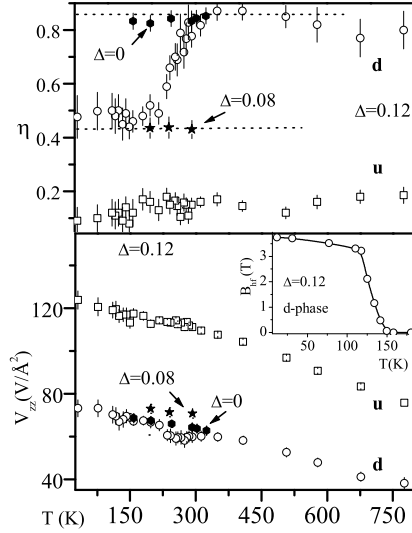


FIG. 2: Asymmetry parameter η (top) and EFG principal component V_{zz} (bottom) for $\text{LaMnO}_{3,12}$ as a function of T . EFG parameters for $\Delta = 0.08$ and $\Delta = 0$ are also showed. Inset: T dependence of the MHF for the d environment.

perature. The MnO_6 octahedra in the R structure are constrained by symmetry to be JT-undistorted (equal Mn-O bond lengths), thus we will name this local environment *undistorted*. In contrast, the d (*distorted*) environment is characterized by a weaker V_{zz} [18] and highly asymmetric EFG ($\eta_d > 0.45$). At high T , the values of η_d and V_{zz}^d coincide with the ones observed for the undoped fully JT-distorted Orthorhombic system, $\Delta = 0$, (full circles in Fig. 2). Consequently, at high temperatures, the d local environment must be characterized by a distortion involving several (minimum eight) Mn^{3+}O_6 octahedra similar to the collective JT-distorted lattice of the orbital ordered LaMnO_3 [19]. Lowering T below 300 K, the asymmetry parameter η_d decreases stabilizing at a value close to that observed for the $\Delta = 0.08$ sample (solid stars in Fig. 2). This behavior suggests that the JT-distortions are weakening till they reach a similar degree as in the $\Delta = 0.08$ sample. The EFG principal components V_{zz}^u and V_{zz}^d slightly increase with decreasing temperature. This is a typical feature of perovskite and related systems [20]. Below $T_c \approx 145$ K both d and u local environments experience increasing magnetic hyperfine fields upon decreasing temperature (inset of Fig. 2), presenting at 10 K values of $B_{hf}^d = 3.8(2)T$ and $B_{hf}^u = 4.0(3)T$ compatible with a full ferromagnetic environment of the surrounding Mn ions [21, 23].

Further insight in the behavior of d and u environments may be achieved by studying the T dependence of the volume fractions f_u and f_d . As may be seen in Fig. 3, the u environment is dominant at very high temperatures ($f_u \approx 86\%$ at $T = 766$ K), though d regions survive up to that T ($f_d \approx 9\%$). This confirms the high stability

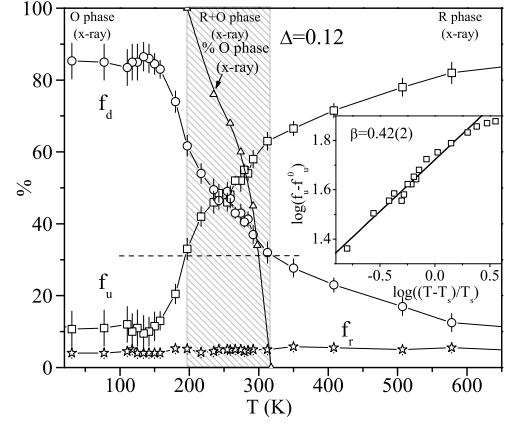


FIG. 3: Temperature dependence of the probe volume fractions f_u , f_d and f_r . Triangles: orthorhombic phase percentage from x-ray diffraction. The shadowed region is limited by the temperatures where the percolation thresholds occur. Inset: log-log plot of $(f_u - f_u^0)$ vs $(T - T_s)$.

of the inhomogeneous phase-segregated state. Our data, at high T , are compatible with a scenario where random distributed JT-distorted nanoclusters are embedded in a undistorted matrix as predicted by [24]. At very low T , the fraction of u environment reaches a remanent value ($f_u^o \approx 10\%$), which is typically observed in CMR manganites [25] and is a signature of the ferromagnetic-metallic (FMM) and FMI phase coexistence. When the temperature changes, f_u (symmetrically f_d) suffers a smooth variation leading from an undistorted to a JT-distorted dominant microscopic environment. If we assume that this variation is a continuous phase transition, the order parameter would be $f_u - f_u^o$ and must follow a power law behavior $f_u - f_u^o \sim (T - T_s)^\beta$ when the critical temperature T_s is approached from above. To check this possibility, we display f_u in a log-log plot in Fig. 3 (inset). The data adjust pretty well to a power law with $T_s \approx 170 \pm 10$ K (relatively close to T_c) and $\beta \approx 0.42 \pm 0.02$. Associated to the transition, there must also exist a correlation length, correlation of the d spatial distribution, that must diverge at T_s . As may be seen in Fig. 2, when T decreases η_d starts to fall as the d component percolates (at $f_d \approx 31.16\%$ [26]) and only stabilizes around T_s . Macroscopically, on the other hand, x-rays measurements detect a structural transition (R - O) that lies exactly between the temperatures corresponding to the percolation thresholds of the two main nanoscopic components. These are precisely the temperatures in which the minority invading cluster suffers a sudden size divergence becoming macroscopically observable.

The temperature dependence of the attenuation of $R(t)$ provides additional information about the dynamics of the u and d environments. A complete sketch of the dynamic and static attenuation for $R(t)$ in both environments is depicted in Fig. 4. The best fit to the $R(t)$

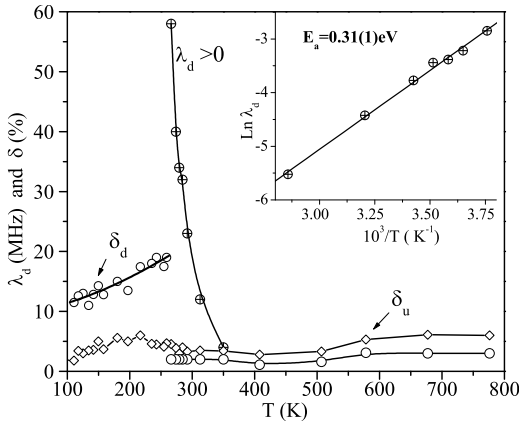


FIG. 4: Temperature dependence of static δ_d (\circ) and dynamic λ_d (\oplus) attenuation parameters to the $R(t)$ function for d environment. Static attenuation δ_u (\diamond) for u environment. Inset: Arrhenius plot of λ_d to estimate the activation energy.

spectra discards the presence of time dependent interactions for the u environment ($\delta_u \approx 4\%$ independently of T and $\lambda_u = 0$). Thus, in all temperature range, the charge transfer between Mn^{3+} and Mn^{4+} (activated hopping) in this environment should occur with a frequency higher than we can probe. For the d environment, on the other side, the best fits were obtained admitting a fluctuating EFG ($\lambda_d \neq 0$ and $\delta_d = 2\%$) in the temperature region spanning from $T = 266\text{ K}$ to $T = 350\text{ K}$. Notice that these time dependent effects cannot be attributed to Cd/O and/or defects diffusion since they would be detected in both fractions. The temperature dependence of the dynamic attenuation parameter, λ_d , allows us to estimate an activation energy E_a . This energy is obtained from $\lambda_d = \lambda_\infty e^{E_a/kT}$, and was found to be $E_a \approx 0.31\text{ eV}$ (see inset Fig. 4), close to the polaron binding energy reported in the literature for low doped manganites [27, 28]. We identify such EFG fluctuations with polaron diffusion related to charge (hole) transport. The EFG fluctuation time (τ) can be estimated from the maximum of $\lambda_d(T)$ [29]. Considering that a carrier (hole) can hop to any of the 8 octahedra around a La site (8 possible EFG states), we find $\tau = 0.5\text{ }\mu\text{s}$ at $T = 266\text{ K}$ corresponding to ultra-slow polaron diffusion. Similar polaron residence times have been recently reported in [21], although the E_a measured there was smaller possibly due to the intense magnetic field (7 T) needed to perform NMR measurements. The competition of the distinct dynamics of the u (fast hopping) and d (related to polaronic conduction) environments is responsible for the macroscopic ferromagnetic insulator behavior observed in these systems [25]. Below T_c , both local environments become ferromagnetic and a phase coexistence between metallic (u) and insulator (d) regions exists. However, the majority fraction (d) is characterized by ultra-slow diffusion of charge carriers imposing an overall insulator behavior.

In conclusion, we report an extensive study on the ferromagnetic insulator manganite $\text{LaMnO}_{3.12}$ using $\gamma - \gamma$ PAC spectroscopy. We analyze in detail the evolution and stability of polaron clusters in an extremely wide range of T that includes a structural transition between R and O phases. PAC measurements reveal a continuous transition between two different dominant local atomic environments (one JT-distorted (d) and another undistorted (u)). Information is also obtained on the local structure, the dynamics and the correlations of these two environments. The macroscopic transition arises as a consequence of the microscopic changes, since it occurs between the percolation thresholds of the two local components. The d environment survives up to very high T where it can be identified with uncorrelated polaron clusters. The correlation of d clusters increases for T below the d percolation threshold diverging at T_s . These results provide further insight in the understanding of the nature/evolution of polaronic distortions and FMM-FMI phase competition responsible for the insulator behavior of these systems.

The authors gratefully thank W. Troeger, U. Wahl, J.M. López, R. Valiente, J. Vieira and R. Catherall for fruitful discussions. This work was funded by the Portuguese Research Foundation (FCT), FEDER (projects POCTI/FN/FNU/50183/03, PDCT/FP/FNU/50145/2003), and EU (Large Scale Facility contract HPRI-CT-1999-00018). J.J.R. received partial funding from the NSF under grant 0312510. A.M.L.L. and E.R. acknowledge their grants to FCT.

* Electronic address: armandina.lima.lopes@cern.ch

- [1] C. Zener *et al.* Phys. Rev. **82**, 403 (1951).
- [2] A.J. Millis *et al.*, Phys. Rev. Lett. **74**, 5144 (1995).
- [3] S.J.L. Billinge *et al.* Phys. Rev. Lett. **77**, 715 (1996).
- [4] G.Zhao *et al.* Nature **381**, 676 (1996).
- [5] D. Louca *et al.* Phys. Rev. B **56**, R8475 (1997).
- [6] V. Kiryukhin *et al.* Phys. Rev. B **67**, 064421 (2003).
- [7] L. Martín-Carrón *et al.* Phys. Rev. B **66**, 174303 (2002).
- [8] N. Mannella *et al.* Phys. Rev. Lett. **92**, 166401 (2004).
- [9] V. Kiryukhin *et al.* Phys. Rev. B **70**, 214424 (2004).
- [10] E. Dagotto, New J. of Physics **7**, 67 (2005).
- [11] C. Ritter *et al.* Phys. Rev. B **56**, 8902 (1997).
- [12] F. Prado *et al.*, J. Sol. Sta. Chem. **146**, 418 (1999).
- [13] J.A.M. van Roosmalen and E.H.P. Cordfunke, J. Solid State Chem. **110**, 109 (1994).
- [14] T. Butz *et al.*, Nucl. Instr. Meth. A **284**, 417 (1989).
- [15] G. Schatz and A. Weidinger, *Nuclear Condensed Matter Physics*, John Wiley & Sons England (1996).
- [16] T. Butz *et al.*, Hyp. Int. **189**, 52 (1989).
- [17] A. Baudry and P. Boyer, Hyp. Int. **35**, 803 (1987).
- [18] Note that the fact that $V_{zz}^d < V_{zz}^u$ alone is not proof enough of a higher symmetry. It has been experimentally observed [20] a sudden decrease in the V_{zz} and increase in η related to a change from a R to a O structure in stoichiometric LaCrO_3 and LaFeO_3 perovskites.

- [19] When the Sternheimer corrections are taken into account, our values for the EFG parameters agree with the results reported in the literature on the undoped compound using NMR [21] and from ab-initio FLAPW theoretical calculations [22]
- [20] R. Dogra *et al.* Phys. Rev. B **63**, 224104 (2001).
- [21] G. Allodi *et al.* Phys. Rev. Lett. **87**, 127206 (2001).
- [22] P. Ravindran, private communication.
- [23] M. K. Gubkin *et al.*, J. Mag. Mag. Mat. **154**, 351 (1996).
- [24] E. Dagotto *et al.* Phys. Reports **344**, 1-153 (2001).
- [25] M.M. Savosta and P. Novak, Phys. Rev. Lett. **87**, 137204 (2001).
- [26] D. Stauffer and A. Aharony, *Introduction to percolation theory*, Taylor & Francis (1992).
- [27] A. Weisse *et al.*, Phys. Rev. B **68**, 024402 (2003).
- [28] J.S. Zhou and J.B. Goodenough, Phys. Rev. B **68**, 144406 (2003).
- [29] H. Winkler and E. Gerdau , Z. Physik.**262**, 363 (1973).